

SCATTERING BY A RIGHT-ANGLED PENETRABLE WEDGE -----  
A STABLE HYBRID SOLUTION (TM CASE)

AUTHOR ASOKE K.BHATTACHARYYA SR. MEMBER,IEEE

ADDRESS Physical Science Laboratory and  
Dept. of Electrical and Computer Eng.  
New Mexico State University  
Box 30002, Las Cruces  
NM 88003-0002

GEOMETRY AND COORDINATE SYSTEM:

The geometry and coordinate system of the structure is shown in Fig.1.

ABSTRACT: The problem of electromagnetic scattering by a dielectric wedge of interior wedge angle  $\pi/2$  has been solved by the hybrid technique combining the Method of Moments(MOM) and Geometrical Theory of Diffraction(GTD) for TM polarization. Pulse functions are used around the edge of the wedge and GTD fields are matched at a distance from the edge on both sides[1]. This substantially reduces the number of MOM current samples to be used. The variation of amplitude and phase of the surface current density has been determined for different values of parameters on both walls. The stability of the matrix solution has been tested. The behaviour of the numerical diffraction coefficient has been discussed. The solution for the scattering from a perfectly conducting wedge is obtained when the relative dielectric constant is equated to a large value (typically, 1000). The attractive feature of this method is that it calls for much less computer memory and also processing time.

NUMERICAL CALCULATIONS,DISCUSSIONS AND CONCLUSIONS:

Numerical calculations were performed using a wide range of the parameters of the problem,namely,the angle of incidence  $\psi_0$ , frequency  $f$ , relative dielectric constant  $\epsilon_r$ ,  $N$ , the number of pulse functions in MM region, GTD matching point distance  $d$  and  $l$ ,the maximum distance in the GTD region. A computer program was prepared in Fortran on the VAX 1680 computer. The parameters  $\psi_0$ ,  $f$ ,  $\epsilon_r$ ,  $N$ ,  $d$  and  $l$  are input quantities. The  $\alpha_m$ 's,  $D_x$ ,  $D_y$ , their amplitude and phase, the stability parameter IER, the variation of amplitude and phase of the surface current density  $J$  on the walls with distance from the edge are output quantities. Provision is also kept to do a parametric study easily. The calculation of near and far fields are not included at the present stage. A typical compilation time was 2.31 sec and an execution time of 0.16 sec for the case of  $\psi_0 = 0$  with 6 MM current pulses and two GTD matching points with  $d = \lambda/4$  and  $l = 5\lambda$ . IMSL routine LEQTLIC was used to solve the matrix equations (8) and (9). The built-in capability of IMSL routine LEQTLIC for testing the stability and singularity of the complex matrix was

utilised. The error parameter IER in the IMSL routine was always zero whereas a value of IER=129 indicates that the matrix is algorithmically singular. Hence, the matrix solution obtained in this study was always stable. The integrals were evaluated numerically by employing a 32 point Gauss quadrature routine. The infinite integrals need be evaluated from d to a suitably chosen l. It is found [11] that a suitable value is  $l=10\lambda$ . This is by virtue of the presence of Hankel function in the integrand.

Fig.2(a)-(d) represent the normalised amplitude and phase of the surface current density on the X-wall with distance along X-walls for different combination of parameters.

In Table 1 are tabulated values of maximum current density and its phase with change in aspect angle for a typical combination of parameters and for  $\psi_0 < 180$  degrees.  $X_c$  is the extent of the pulse current from the edge and N is the number of pulses used.

Table 2 gives the variation of real and imaginary parts of  $D_x$  and  $D_y$  with aspect angle for a typical combination of parameters and for  $\psi_0 < 180$  degrees. The effect of dielectric loss on the numerical diffraction coefficient and maximum current density and their phase for a typical situation with  $f=10$  GHz;  $N=10$ ;  $\psi_0 = 120$  degrees;  $\epsilon_R = 4.0$  is illustrated in Table 3.

Table 1

MAXIMUM CURRENT DENSITY WITH ASPECT ANGLE

$f=10$  GHz;  $N=10$ ;  $\epsilon_R=4.0$ ;  $d=X_c$ ;  $X_c = 2\lambda / 5$ ;  $l=6\lambda$ .

Aspect angle in degrees	Current density in amp/m.
0.0	1.9819
22.5	1.8685
45.0	1.5304
67.5	0.8204
90.0	0.2934
112.5	1.4261
135.0	3.2987
157.5	5.8636
180.0	7.3397
202.5	5.8636
225.0	3.2987
247.5	1.4260
270.0	0.2930

Table 2

VARIATION OF  $D_x$  AND  $D_y$  WITH ASPECT ANGLE  
 $f=10$  GHz.;  $N=10$ ;  $\epsilon_R=4.0$ ;  $d=X_c$ ;  $X_c=2\lambda$ ;  $l=6\lambda$ .

Aspect angle in degrees.	$D_x$		$D_y$	
	Real Part	Imag. Part	Real Part	Imag. Part
0.0	0.261E-03	-0.249E-02	-0.414E-04	0.125E-01
22.5	0.901E-04	-0.179E-02	0.117E-02	0.124E-01
45.0	-0.815E-03	-0.841E-03	0.112E-01	0.309E-02
67.5	0.295E-02	0.465E-03	0.991E-03	-0.521E-02
90.0	0.996E-02	0.291E-02	-0.157E-01	0.462E-02
112.5	0.295E-02	0.465E-03	0.991E-03	-0.522E-02
135.	-0.815E-03	-0.841E-03	0.112E-01	0.309E-02
157.5	-0.91E-04	-0.179E-02	0.117E-02	0.124E-01
180.0	-0.261E-04	-0.249E-02	-0.414E-02	0.124E-01
202.5	-0.901E-04	-0.179E-02	0.117E-02	0.124E-01
225.0	-0.815E-03	-0.841E-03	0.112E-01	0.309E-02
247.0	0.294E-02	0.465E-03	0.991E-03	-0.521E-02
270.0	0.996E-02	0.291E-02	-0.158E-01	0.462E-02

The effect of dielectric loss on the numerical diffraction coefficient and maximum current density and their phase for a typical situation with  $f=10$  GHz;  $N=10$ ;  $\psi_0=120$  degrees;  $\epsilon_R=4.0$  is shown in Table 3.

Table 3

Effect of Dielectric Loss on Current Density, its Phase and Numerical Diffraction Coefficients.

$F=10$  GHz.;  $\psi_0=120$  deg.;  $N=10$ ;  $N_1=12$ ;  $\epsilon_R=4.0$ ;  $X_c=2\lambda$ ;  $l=6\lambda$ ;  
 $d=X$  .

D		D	
w/o loss	with loss	w/o loss	with loss
(0.617, -0.272)	(0.572, -0.375)	(0.765, -0.535)	(0.675, -0.662)
E-03	E-03	E-02	E-02
Max. current density		Phase of Max.J	
w/o loss	with loss	w/o loss	with loss
1.9373	1.9781	-0.35	-14.00

Figs. 3(a)-3(d) show the variation of  $|D_x|$ ,  $|D_y|$ , maximum  $|J|$  and its phase  $\angle J$  with relative dielectric constant for  $X_c = \lambda/2$ ,  $D=3\lambda/4$ ,  $l=5\lambda$  and  $N=4$ . It is found that all the

variations are linear functions of  $\epsilon_R$ . For low values of  $\epsilon_R$  the variations have been found to be nonlinear.

Fig. 4(a) and 4(b) respectively give the behaviour of magnitude and phase of the current density with incident angle for complete  $2\pi$  variations. The change in the magnitude of the current density is rather small but the phase varies from  $-90$  to  $+90$  degrees rapidly in the range of  $2\pi$  radians.

In Fig.5 is shown a particular case where  $\epsilon_R$  is equated to 1000 to simulate a perfectly conducting wedge. This field decay is compared with the exact solution available in [1] in Fig.5. The agreement seems to be reasonable.

In conclusion, the problem of electromagnetic scattering by a right-angled lossy dielectric wedge has been formulated. The numerical diffraction coefficients can be obtained by this method. The surface current density on the walls have been plotted.

COMPUTER CODE: DW.FOR

COMPUTER MODEL : VAX

MEMORY REQUIREMENTS AND SOLUTION TIME:

REFERENCES:

[1] W.D. Burnside, C.L.Yu and R.J. Marhefka - 'A Technique To Combine The Geometrical Theory Of Diffraction and The Moment Method', IEEE Trans. Antennas and Propagat., Vol AP-25, July 1975, pp. 551-558.

Legends to the Illustrations:

Fig.1: Electromagnetic scattering of a TM wave by a 90 degree wedge.

Fig.2: Variation of amplitude and phase of the current density along x-wall.

- (a)  $N=8; X_c = 2\lambda/5; D = \lambda/2; l=100$  ;  $\psi_0 = 0$  degree.  
 (b)  $N=4; X_c = \lambda/2; D=3. \lambda/4; l=5$  ;  $\psi_0 = 120$  degree.  
 (c)  $N=4; X_c = \lambda/2; D=3. \lambda/4; l=5$  ;  $\psi_0 = 180$  degree.  
 (d)  $N=8; X_c = 2\lambda/5; D = \lambda/2; l=100$  ;  $\psi_0 = 270$  degree.

Fig.3: Variation of  $|D_x|$ ,  $|D_y|$ ,  $\text{Max}(|J|)$  and  $\angle J$  with dielectric constant.

- (a)  $|D_x|$  and  $|D_y|$  (b)  $\text{Max}(|J|)$  and  $\angle J$  ;  $f=10$  GHz;  $\psi_0 = 120$  degrees;  $D = 3 \lambda/4$ .;  $l=5\lambda$  ;  $N=4$ ;  $Nl=6$ .

Fig.4: Amplitude and phase of the total surface current density on the x-wall for different values of incident angle .(a) amplitude (b) phase;

$$f=10 \text{ GHz}; \epsilon_R = 2.56; d=3\lambda/4; l=5\lambda; N=6; Nl=8.$$

Fig.5: Comparison of the surface current density from this formulation with a perfectly conducting wedge solution.

$$N=8; X_c = 2\lambda/5; f=10 \text{ GHz}; \epsilon_R = 1000; \tan\delta = 0.0$$

\_\_\_\_\_ Results with present theory  
 x x x x Perfectly conducting wedge solution[1].

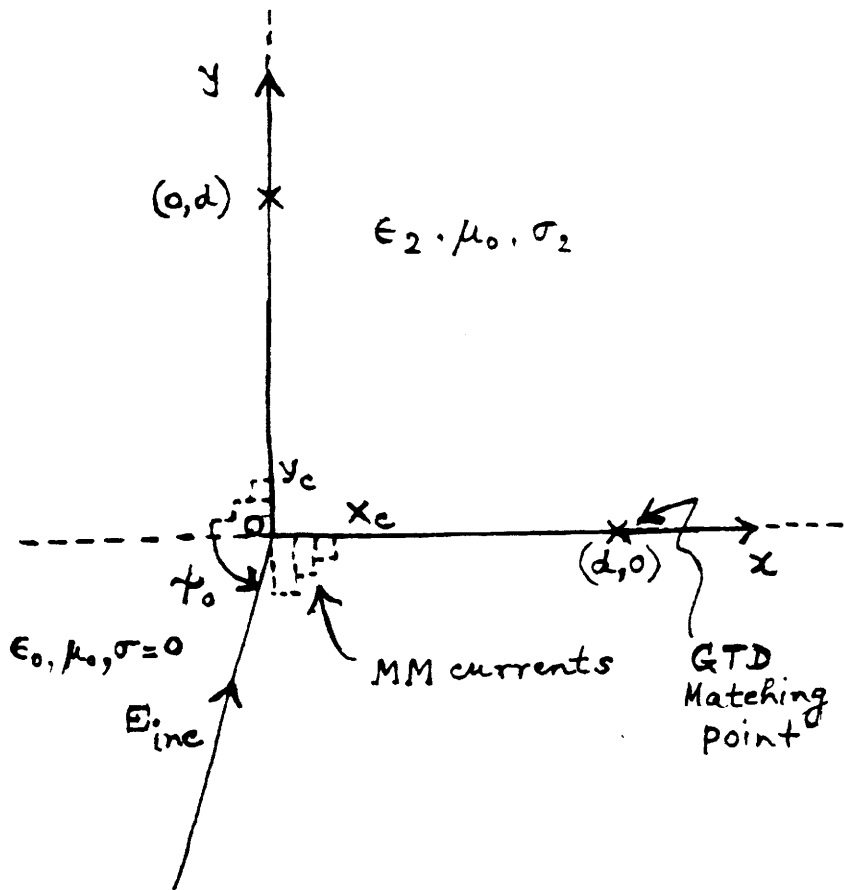
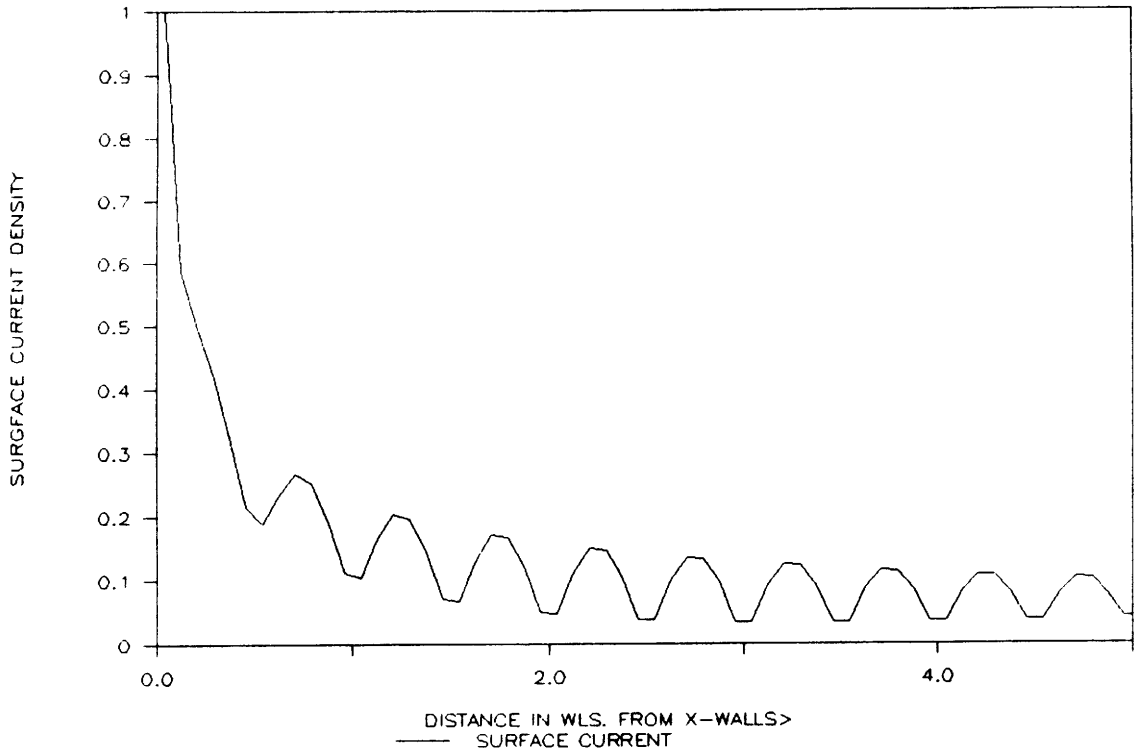


Figure 1

# DW6.PRN;SURFACE CURRENT DENSITY

EPSR=2.56;N=8;F=10GHz;XC=2WL/5;D=WL/2;



# DW61.PRN;SURFACE CURRENT DENSITY

EPSR=2.56;N=8;F=10GHz;XC=2WL/5;D=WL/2;

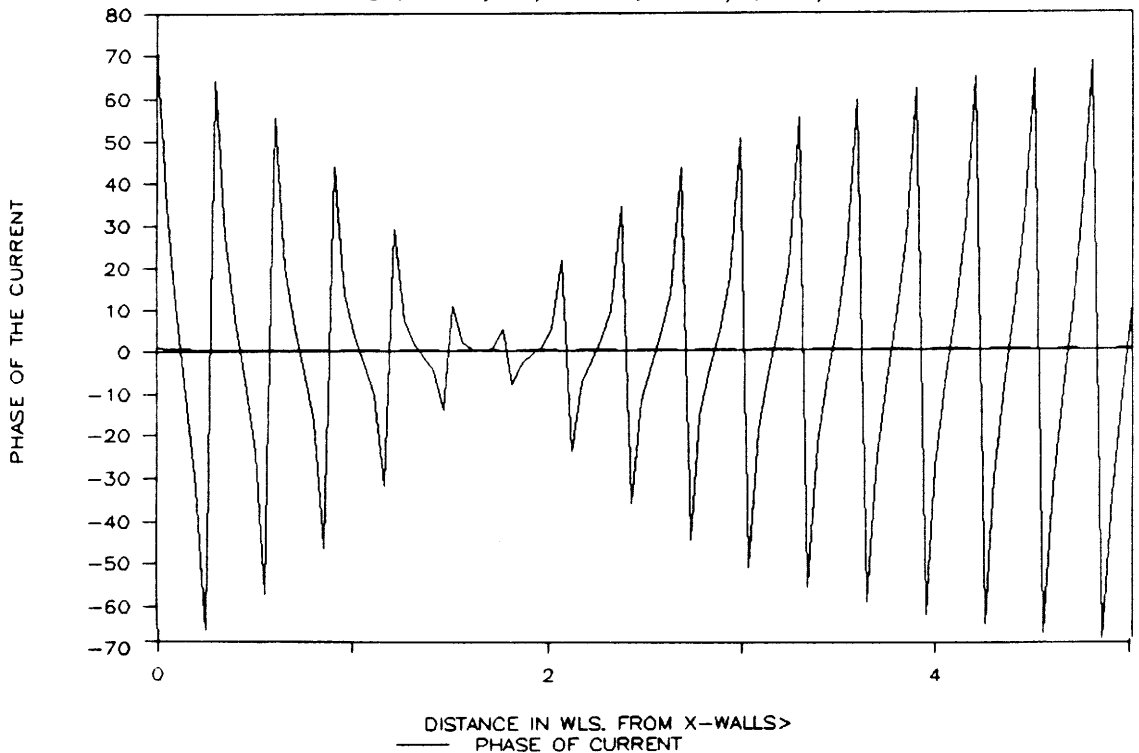
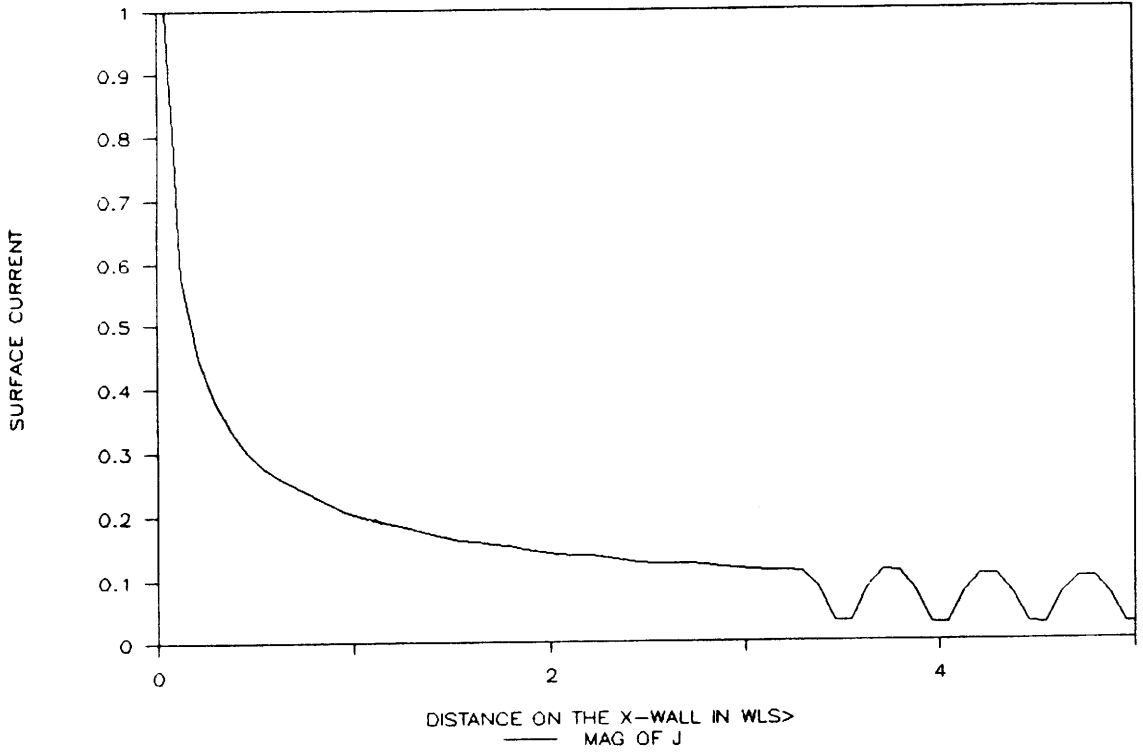


Figure 2(a)

# SURFACE CURRENT

EPSR=4;F=10;SID=270;N=8;D=WL/2;XC=2WL/5



DW41;N=4;XC=WL/2;D=3WL/4;L=5WL; $\psi_0=120$ DEG

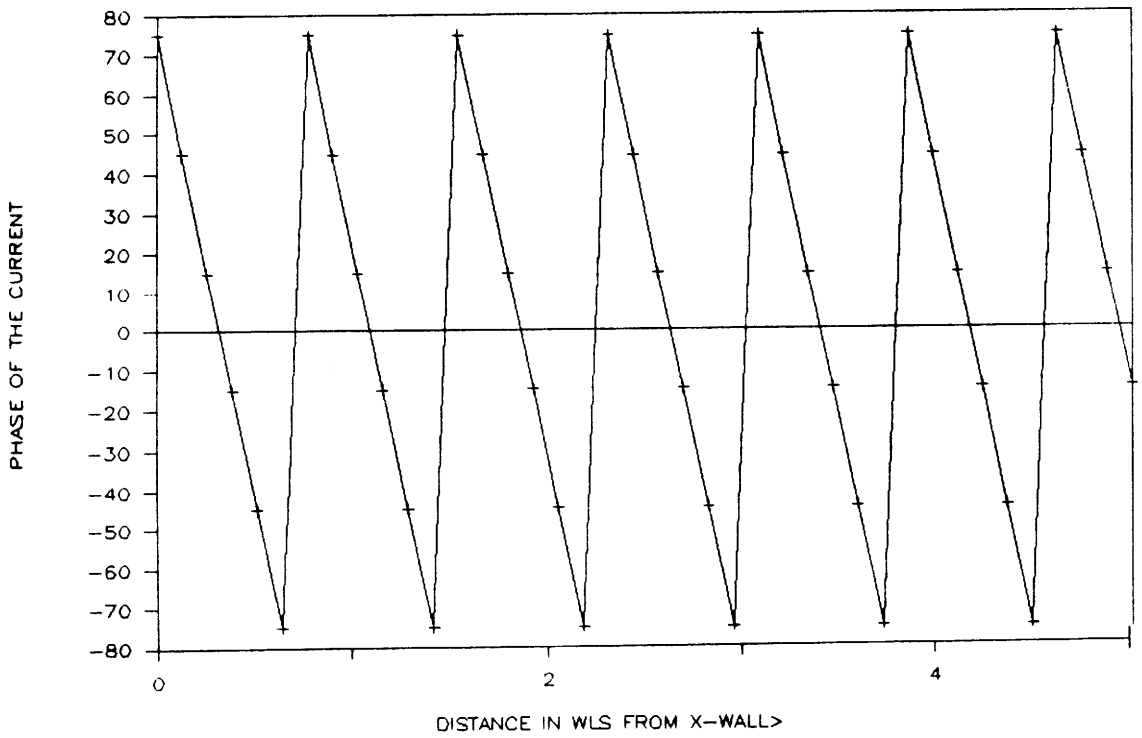
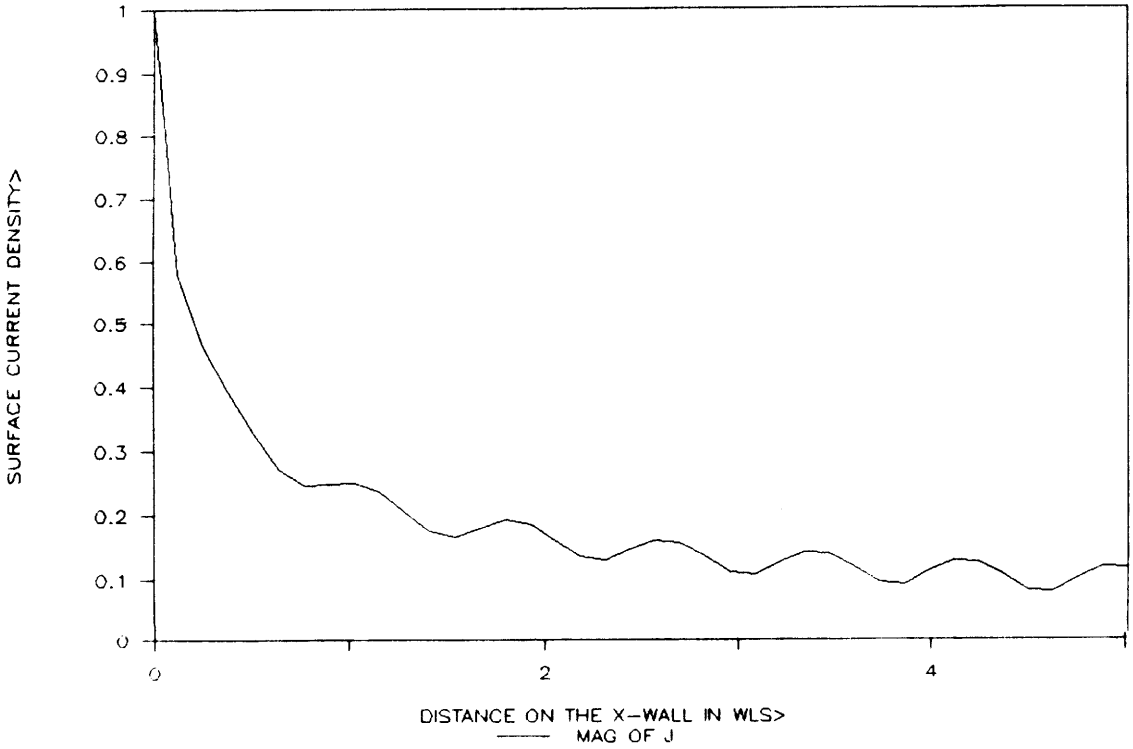


Figure 2(b)



# DW8; SURFACE CURRENT

$N=4; X_C=WL/2; D=3WL/4; L=5WL; S_1=180 \text{ DEG};$



# DW81

$N=4; X_C=WL/2; D=3WL/4; L=5WL; \psi_0 = -180 \text{ DEG};$

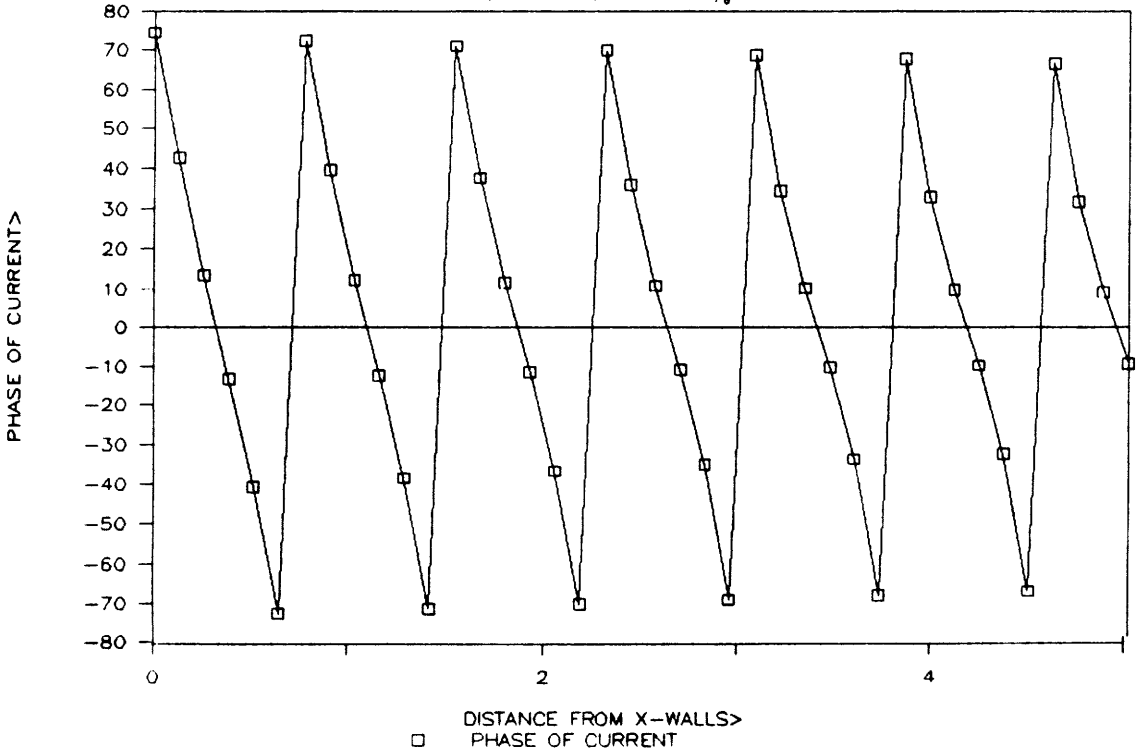
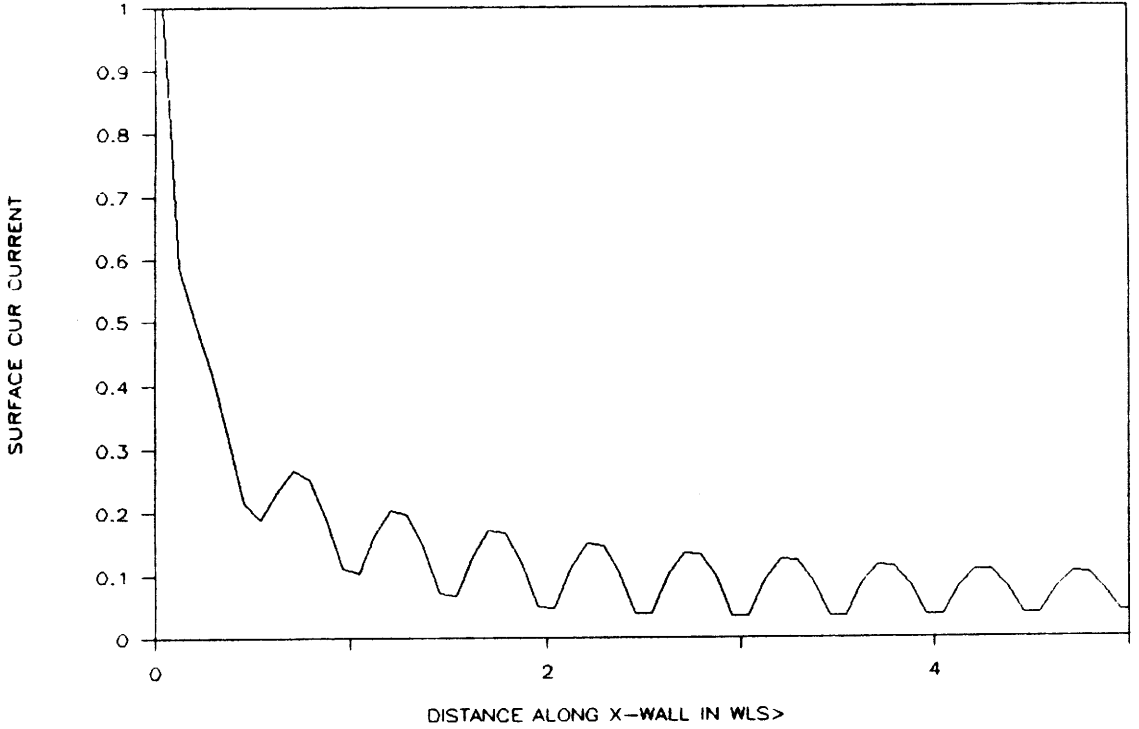


Figure 2(c)

# DW9;SURFACE SURFACE DENSITY

N=8;XC=2WL/5;D=WL/2;L=100WL;SI=270 DEG;



# DW91;PHASE OF CURRENT

N=8;XC=2WL/5;D=WL/2;L=100WL;  $\psi_0 = 270$  DEG

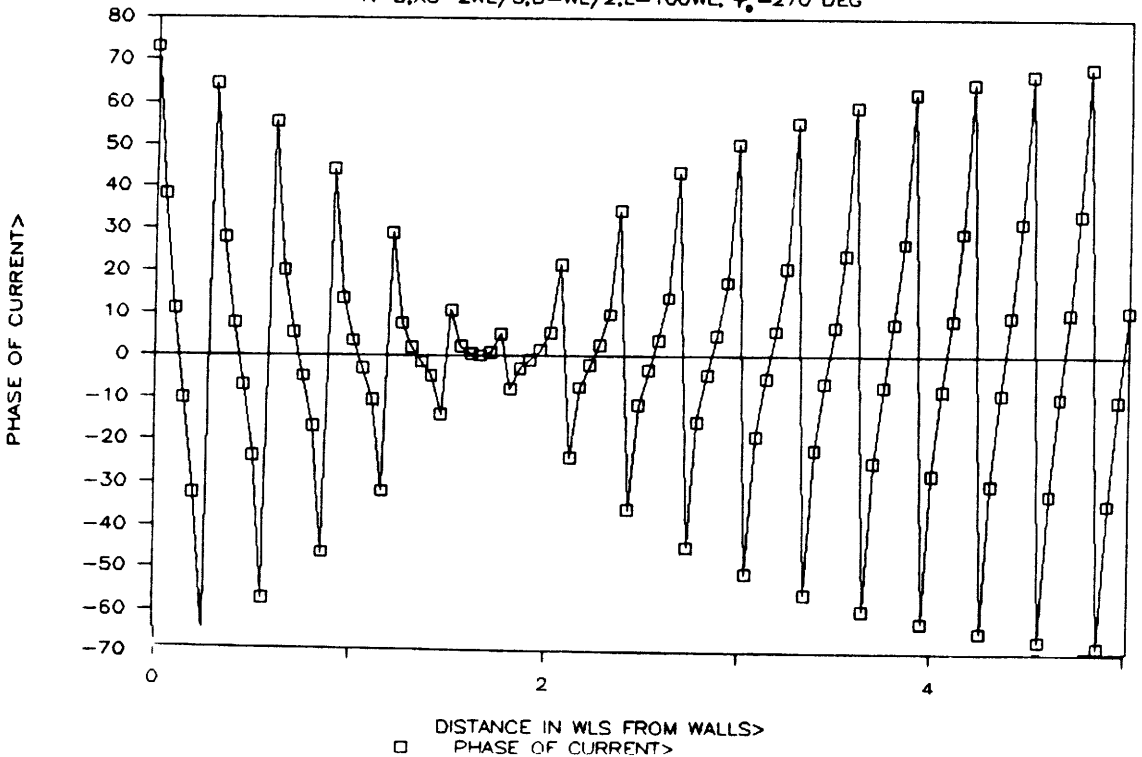


Figure 2(d)

# DW12; MAGNITUDES OF Dx AND Dy

EPSR=2.56;F=10GHz;D=3WL/4;L=5WL;N=6;

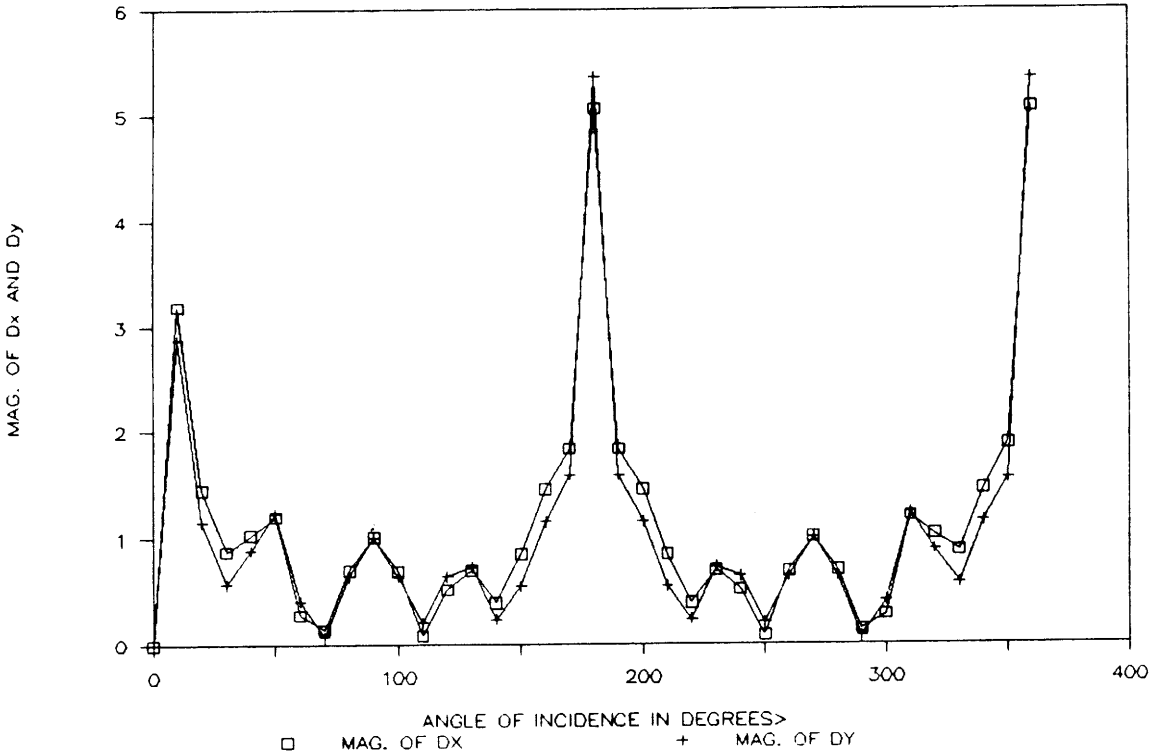


Figure 3(a)

# DW13; MAX. OF J AND PHASE OF J

EPSR=2.56;F=10GHz;D=3WL/4;L=5WL;N=6;

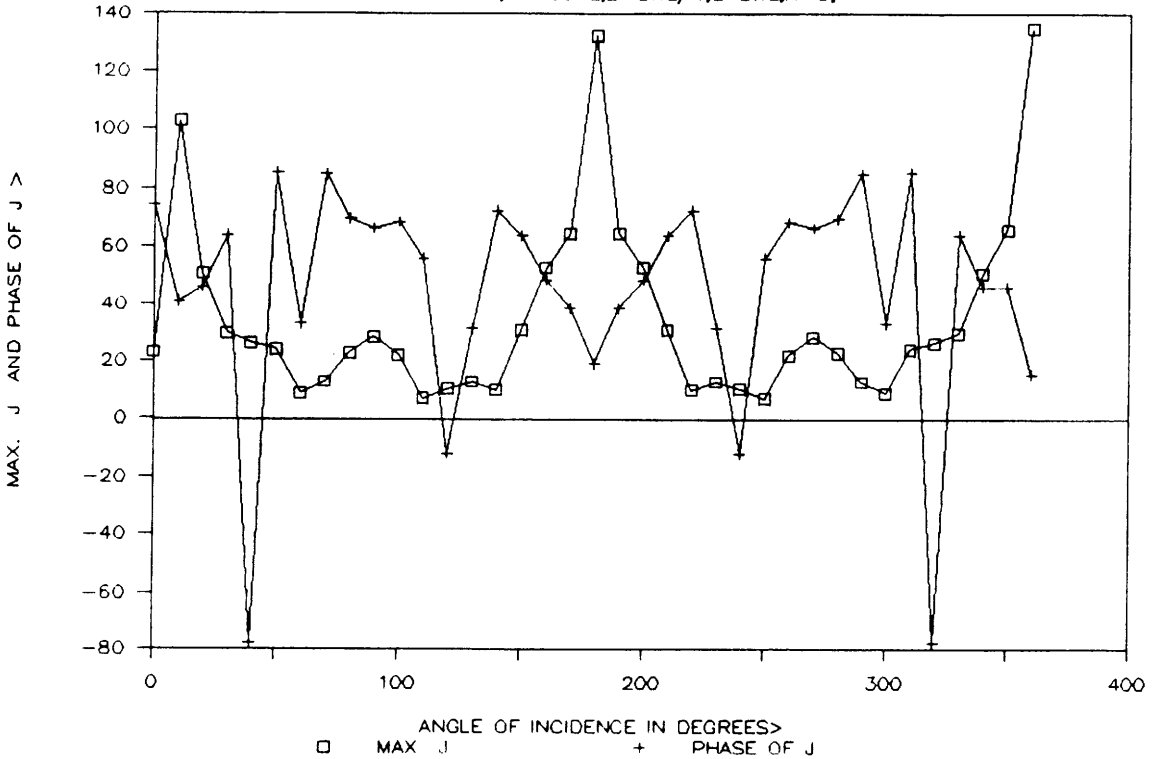


Figure 3(b)

# DW10; D<sub>x</sub> AND D<sub>y</sub> VS. DIELECTRIC CONSTANT

N=4; F=10GHz; D=3WL/4; L=5WL; SI=120;

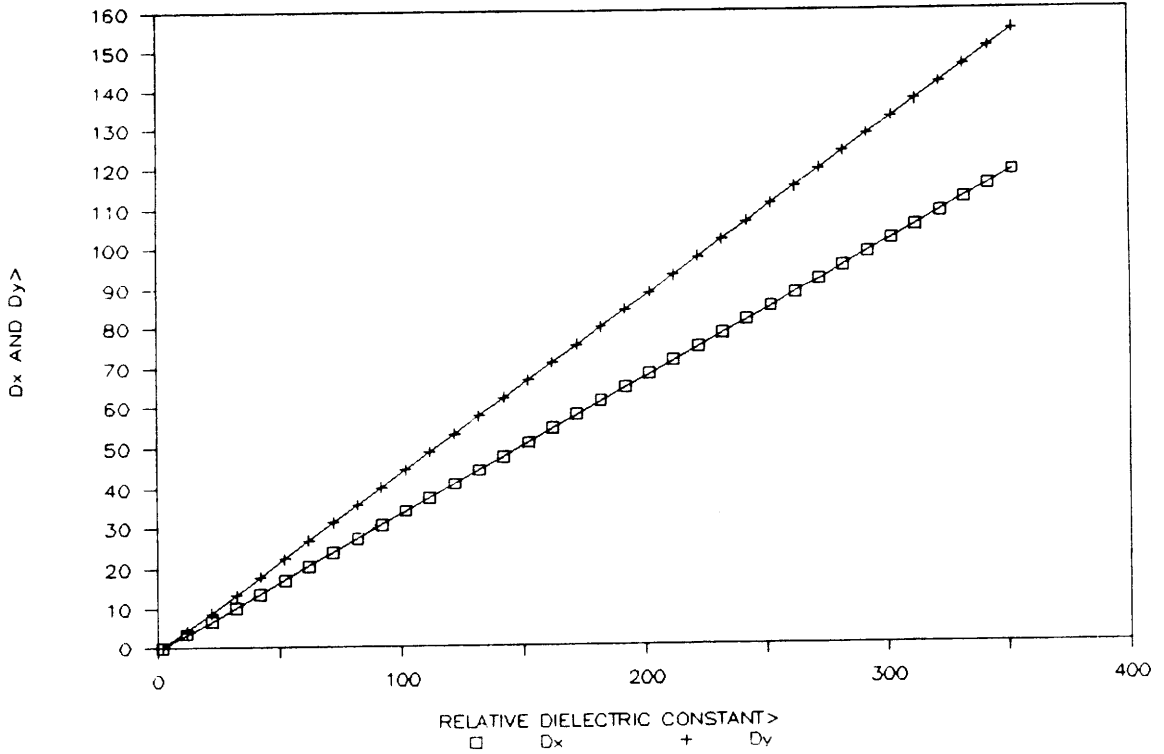


Figure 4(a)

# DW11; MAX. J AND ITS PHASE

F=10GHz; N=4; L=5WL; D=3.WL/4; SI=120;

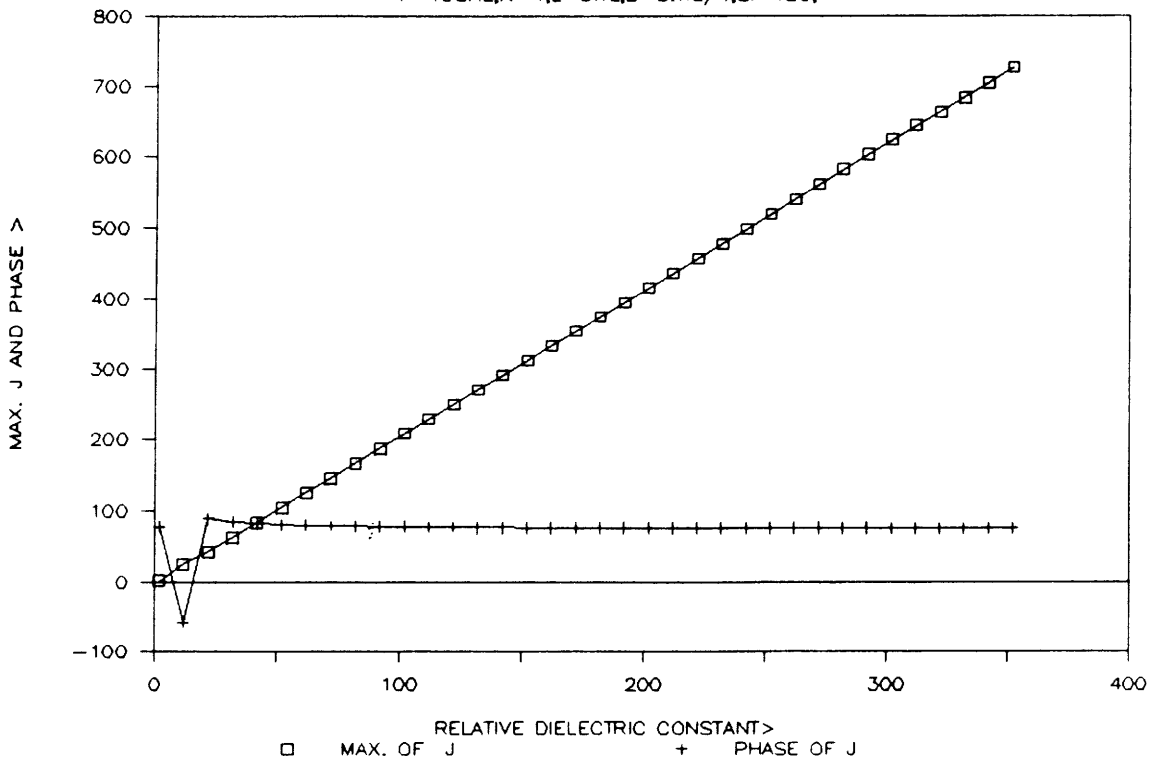


Figure 4(b)

# DW2; SURFACE CUR DENSITY

N=8;XC=2WL/5;D=WL/2;L=100WL; SID=270;

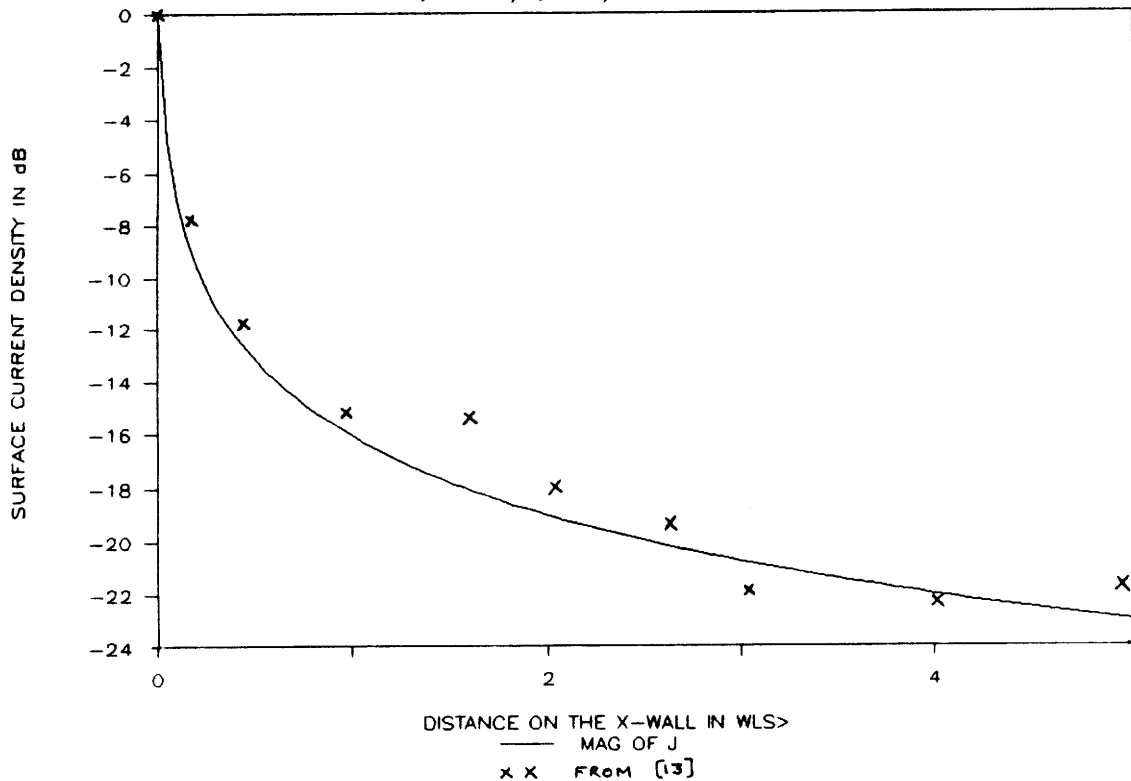


Figure 5(a)

# DW21; PHASE PLOT

N=8;XC=2WL/5;L=100WL;F=10GHZ;SI=270;

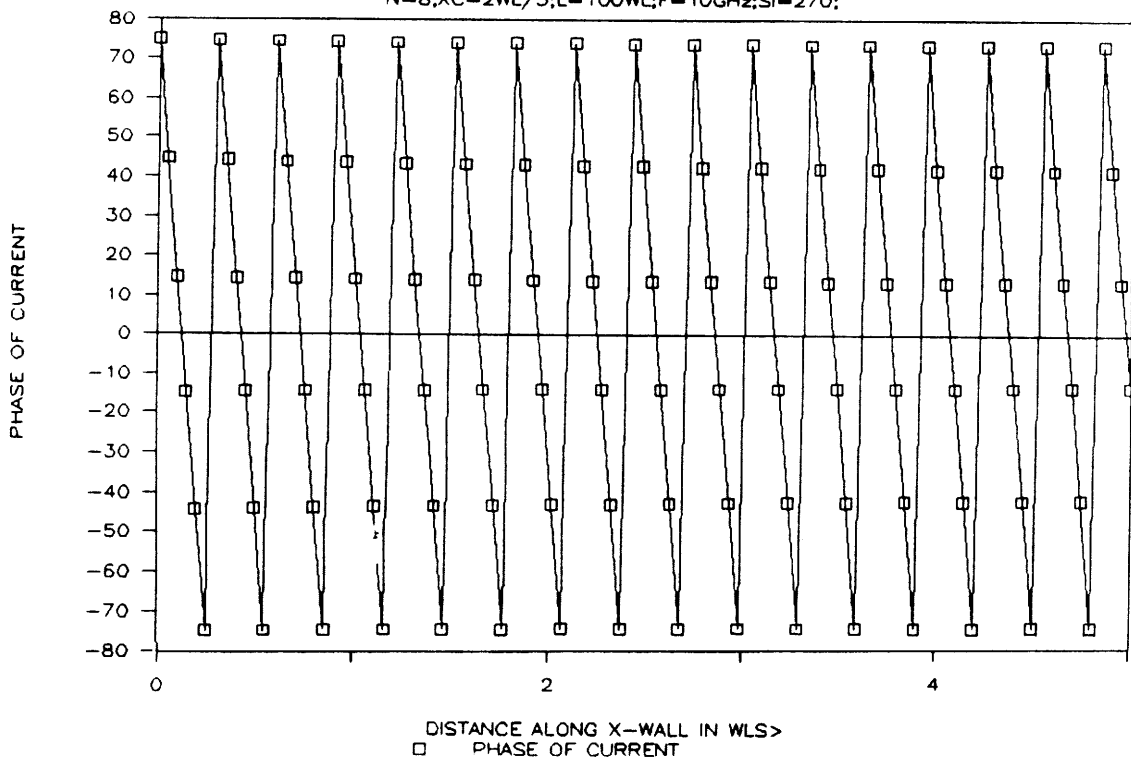


Figure 5(b)